

Unifying Logarithmic And Factorial Behavior in High Energy Scattering

J.M. Cornwall* and D.A. Morris*

University of California, Los Angeles
405 Hilgard Ave., Los Angeles, CA 90024, U.S.A.

Abstract

The elegant instanton calculus of Lipatov and others used to find factorially-divergent behavior ($g^N N!$) for $Ng \gg 1$ in $g\phi^4$ perturbation theory is strictly only applicable when all external momenta vanish; a description of high-energy $2 \rightarrow N$ scattering with N massive particles is beyond the scope of such techniques. On the other hand, a standard multiperipheral treatment of scattering with its emphasis on leading logarithms gives a reasonable picture of high-energy behavior but does not result in factorial divergences. Using a straightforward graphical analysis we present a unified picture of both these phenomena as they occur in the two-particle total cross section of $g\phi^4$ theory. We do not attempt to tame the unitarity violations associated with either multiperipheralism or the Lipatov technique.

UCLA 94/TEP/31

August 1994

*cornwall@physics.ucla.edu

*dmorris@physics.ucla.edu

1 Introduction

There is a long-standing problem in high-energy scattering which could have been addressed over a decade ago but was not, apparently for a lack of applications. The problem resurfaced a few years ago in a mutated form when Ringwald[1] and Espinosa[2] pointed out that a strict application of the standard dilute-instanton-gas approximation (DIGA) in the electroweak standard model leads to large $B + L$ -violating cross sections for $2 \rightarrow N$ scattering when $N \gtrsim O(1/\alpha_W)$ (that is, at energies $\gtrsim O(M_W/\alpha_W) \simeq$ sphaleron mass[3]). Shortly thereafter one of us pointed out[4] that the same DIGA, in the remarkable application of Lipatov[5] and others[6] to finding the terms of large-order perturbation theory[7], gives the wrong high-energy behavior to purely perturbative processes essentially because the DIGA cuts off instanton size scales in the infrared by masses and not by characteristic energies.

The Lipatov-DIGA provides a convenient means of obtaining factorially divergent matrix elements $T_{2 \rightarrow N}$ (for $N \gg 2$) which ultimately need to be tamed by unitarity or, where applicable, Borel summation[8]. In this paper we will not be concerned with how these divergences are brought under control, which is an interesting and important issue by itself, but rather we will concentrate on their energy dependence — an aspect which the Lipatov-DIGA is not well suited to address.

The shortcomings of the Lipatov-DIGA become evident if one considers the dependence of $T_{2 \rightarrow N}$ on the center of mass scattering energy E . When E and the average energy per outgoing particle, E/N , are large compared to all masses involved, one anticipates that $T_{2 \rightarrow N}$ should scale like E^{2-N} (aside from logarithms and N -dependent factors). However, in the Lipatov-DIGA $T_{2 \rightarrow N}$ scales like M^{2-N} for some fixed mass M , even if $E/N \gg M$. The suspicious energy-independence of the basic Lipatov-DIGA calls into question the rôle of energetic external particles in factorially divergent scattering amplitudes and leads one to ask how such amplitudes can co-exist with energy-dependent amplitudes which do not diverge factorially. In this paper we present a unified analysis of this problem based on conventional Feynman diagram techniques which demonstrate the emergence of factorially divergent amplitudes and their interplay with familiar energy-dependent amplitudes.

For definiteness, we will study the two-particle total cross section in a theory characterized by the interaction Lagrangian $\mathcal{L}_I = -g\phi^4/4!$. In particular, we will concentrate on the imaginary part of the forward scattering amplitude $Im T_{2 \rightarrow 2}(t = 0, s \gg m^2)$ which is related to the two-particle total cross section through unitarity. In addition to introducing a class

of amplitudes whose sum exhibits factorially divergent behavior we will also consider the consequences of amplitudes with high-energy infrared (IR) logarithms (few graphs, but with many partial waves) which profoundly alter the overall energy dependence. These IR logarithms, associated with the occurrence of many propagators with small momentum transfers arise from graphical analyses much older than the Lipatov approach: multiperipheralism[9].

The study of multiperipheral graphs like the uncrossed ladder graph of Fig. 1 is based on considering large orders of perturbation theory with an emphasis on summing leading infrared logarithms which eventually appear as sums of powers of $g \ln(s/m^2)$. Contributions of N^{th} order ladder graphs to $\text{Im } T_{2 \rightarrow 2}(t = 0, s \gg m^2)$ are not accompanied by a factor of $N!$ but rather by a factor of $1/N!$ and these sum to give[10, 11]

$$\text{Im } T_{2 \rightarrow 2}(s \gg m^2, t = 0) \sim \frac{g^2}{\ln^{3/2}(s/m^2)} \left[\left(\frac{s}{m^2} \right)^{g/(16\pi^2)} + (g \rightarrow -g) \right]. \quad (1)$$

The term with the sign of g reversed ensures that only even powers of g appear in the final answer. In contrast to ladder graphs, the class of graphs which we will introduce, whose sum gives $N!$ behavior, is free from logarithms.

The characteristic features of $g\phi^4$ diagrams without logarithms in their imaginary part are the absence of multiple lines between vertices and the absence of lines beginning and ending on the same vertex (tadpoles). In graph-theoretic language such diagrams are known as “simple graphs”. In section 2 we introduce a subset of simple graphs which we call K –graphs whose properties are easily understood since they are straightforward generalizations of multiperipheral graphs; they have neither infrared nor ultraviolet logarithms in their imaginary part. A crucial part of our analysis is a factorization theorem, stated in Section 3 and proved in appendix D, which allows us to isolate the contribution of simple graphs from diagrams where they mix with ladder graphs. Though we illustrate the factorization theorem using K –graphs, the theorem holds for all simple graphs.

Using factorization to combine simple graphs with ladder graphs gives an extremely concise result: in the analysis of ladder graphs one effectively makes the substitution

$$g \rightarrow g \left(1 + \sum_{\text{even } N} \left(\frac{ag}{16\pi^2} \right)^N N! \right)^{1/2} \quad (2)$$

where the sum on the right-hand side is recognized as being factorially divergent. Specifically, Eq. 1 is modified to

$$\text{Im } T_{2 \rightarrow 2}(s \gg m^2, t = 0) \sim \frac{g^2 \beta(g)}{\ln^{3/2} \left(\frac{s}{m^2} \right)} \left[\left(\frac{s}{m^2} \right)^{\alpha(g)} + (g \rightarrow -g) \right], \quad (3)$$

where

$$\beta(g) = \left(\frac{16\pi^2}{g} \alpha(g) \right)^2 \doteq 1 + \sum_{\text{even } N} \left(\frac{ag}{16\pi^2} \right)^N N! . \quad (4)$$

The difference between considering just K -graphs or all simple graphs amounts to different estimates for the constant a . Including only K -graphs we find the bound $a_K \geq 1/2$ and we estimate $a \simeq 0.94$ if all simple graphs are included; the corresponding Lipatov value is $a = 1$. The difference between our estimates and the Lipatov value likely reflects the fact that our graphical sum of contributions to $Im\ T_{2 \rightarrow 2}$ is not exhaustive.

In Eq. 4 we have introduced a modified equality sign \doteq which we use throughout the paper. Two N -dependent functions A_N , B_N (or sums of such functions) obey $A_N \doteq B_N$ if, for large N , A_N and B_N are of the form $c_1(N!)^{c_2} c_3^N N^{c_4} (1 + O(1/N))$ with c_2 and c_3 being the same constants for both A_N and B_N . That is, overall constant factors, fixed powers of N , and non-leading terms are ignored, and may differ from A_N to B_N .

For non-forward scattering ($t \neq 0$) the terms in the sum of Eq. 4 have extra factors $F_N(t)$, with $F_N(0) = 1$, which are calculable in principle with our technique, but we will not consider the case $t \neq 0$ here. Note, by the way, that we only treat graphs corresponding to even powers of g whereas the Lipatov analysis treats both even and odd powers. Consequently, $(-1)^N$ factors which would normally appear in a sum like Eq. 4 have no effect.

One might think that the result of Eqs. 3-4 is obvious and, in a rather hand-waving way, it is. The problem, however, is to find a way to derive it and we know of no direct application of the Lipatov technique for doing this. Our approach simply involves summing graphs, sometimes using the Bethe-Salpeter equation. Though there are many regularities in our analysis which suggest an underlying semi-classical behavior, we cannot yet assemble these clues into a Lipatov-like semi-classical derivation of our results.

The difficulty in obtaining the true high-energy behavior from Lipatov theory can be traced to the fact that the Lipatov-DIGA analysis is, in principle, only applicable to graphs with zero four-momentum on every external leg[12]. This is a consequence of the vanishing of all the matrix elements of the semi-classical energy momentum tensor when evaluated on the Lipatov instanton-like solutions of wrong-sign $g\phi^4$ theory. One might hope that summing quantum corrections to the basic DIGA result will make it possible to derive high-energy results, but so far work[13] on the analogous problem of high-energy B+L violation has not yet resolved this problem. What is needed for the semi-classical analysis to succeed at high energy is to find a means of communicating the energy of the external on-shell particles to the instantons, a feat which is most easily accomplished in Minkowski space. Otherwise,

the instantons and analogous objects in the Lipatov analysis can be of any size and, when all sizes are integrated over, the M^{2-N} behavior for $T_{2 \rightarrow N}$ emerges, as mentioned earlier. There has been speculation as to how information on external energies can be transferred to the instantons by solving inhomogeneous instanton equations with external-particle energy-dependent sources[12] but exact solutions of the relevant equations do not exist with the necessary generality.

In the graphical approach, all graphs begin with the appropriate on-shell high-energy external lines attached. Certain graphs, or parts of graphs, can be factored out or otherwise identified in the overall process, which have the property that they are independent of the external momenta, at least for forward scattering; such graphs look very much like graphs with all four-momentum vanishing even though they are Minkowski-space high-energy graphs, or parts thereof. It is these graphs which contribute to α , β and the $N!$ behavior of Eq. 3. They are also the graphs for which we would expect some sort of semiclassical analysis to hold, but as mentioned above we do not know how to do this at the level of $Im\ T_{2 \rightarrow 2}$ itself.

An interesting problem for the future would be to find a semiclassical analysis for $Im\ T_{2 \rightarrow 2}$ at high energy. A non-trivial extension of the present paper is to generalize the results on $Im\ T_{2 \rightarrow 2}$ to multiloop graphs for $T_{2 \rightarrow N}$. The most challenging problem is to extend the results to gauge theories, where new complications arise. In $g\phi^4$ theory the reduced graphs contributing to α and β of Eq. 3 are four-dimensional while in gauge theory they are two-dimensional[14]. Since there are infinitely many conformally invariant two-dimensional theories, there is no standard Lipatov analysis for such theories. Recently, there has been speculation[15] on the form of this two-dimensional theory for non-abelian gauge theories and gravity in four dimensions, but the problems of incorporating the correct high-energy behavior (i.e., the leading logarithms) has only begun to be addressed in this context. We will briefly discuss these problems for the future in the concluding section.

The outline of the paper is as follows. In Sect. 2 we identify a class of diagrams which generalizes the notion of multiperipheral graphs and we demonstrate that their contribution to $Im\ T_{2 \rightarrow 2}$ gives rise to an energy-independent $N!$ behavior analogous to that found by Lipatov-DIGA techniques. We call the generalized graphs K -graphs since we eventually use them to define a kernel for a Bethe-Salpeter equation. The statistical picture which emerges in Sect. 2 brings to mind the work of Bender and Wu[16] and Parisi[17]. Our analysis goes beyond previous studies in that we keep track of the manner in which K -graphs exhibit factorial divergences so that we can later merge them with energy-dependent amplitudes. In Sect. 3 we form chains of K -graphs and two-line loops (which by themselves are responsible

for leading-log behavior) and sum them to obtain the result of Eqs. 3-4. We uncover a factorization theorem which reduces the problem of summing chains of K -graphs and two-line loops to the well-studied problem of summing straight-ladder graphs. Details of our calculations are given in Appendices A-E.

2 Graphical Analysis

2.1 Choice of Graphs

Consider the uncrossed ladder graph of Fig. 1. Since there is only one such graph in the N^{th} order of perturbation theory its statistical weight can not contribute to the $N!$ behavior of $\text{Im } T_{2 \rightarrow 2}$. Nevertheless, the imaginary part of this graph has the maximum possible powers of $\ln(s/m^2)$ (which is $N-2$ in N^{th} order). Here m is the mass of the particle propagating in the vertical lines of Fig. 1; one can safely ignore all other masses without encountering additional IR divergences and we will do so whenever possible. In particular, we take $p^2 = p'^2 = 0$. Since Fig. 1 is essentially the square of a tree graph, it will not contribute UV logarithms to $\text{Im } T_{2 \rightarrow 2}$ (though it contributes a single UV logarithm to $\text{Re } T_{2 \rightarrow 2}$).

One can generalize the notion of multiperipheral graphs by drawing two opposing trees as in Fig. 2 (corresponding to a $2 \rightarrow N$ contribution to $\text{Im } T_{2 \rightarrow 2} \sim \sum |T_{2 \rightarrow N}|^2$) and then joining the lines on one tree to the lines on the other in all possible ways. Among the graphs formed in this manner are uncrossed ladder graphs like Fig. 1 (which have many two-line loops), graphs like Fig. 3a (which have no two-line loops), crossed ladder graphs like Fig. 4a, and graphs such as those of Fig. 5 (which include graphs with a few two-line loops). In this paper we will restrict our attention to two types of graphs and a certain way of intertwining them. The first type of graph is the familiar uncrossed ladder of Fig. 1 while the second type has as its simplest example the graph of Fig. 5a. The defining features of graphs like Fig. 5a are the absence of two-line loops and two-particle irreducibility in t (vertical) channel.

An algorithm for constructing N^{th} order graphs like Fig. 5a begins by marking each of two vertical lines with $N/2$ vertices (N is even for all our graphs) as in Fig. 2. One then takes a closed loop of string and attaches it to the vertices in such a way that in tracing the string one alternately goes from one vertical line to the other without revisiting any vertex. We will call graphs constructed in this manner K -graphs; Fig. 3a is an example of an eighth-order K -graph. In Sect. 2.3 we show that there are $O(N!)$ K -graphs in the N^{th} order of perturbation theory and that, due to their lack of two-line loops, K -graphs contribute no logarithms to $\text{Im } T_{2 \rightarrow 2}$. Among the graphs we exclude by concentrating on K -graphs are

graphs like Fig. 4a (which has fewer logarithms than the corresponding uncrossed ladder graph) and Fig. 4b (which has UV logs). We also exclude graphs like Fig. 5c which may affect the details of our quantitative results but which do not change the overall picture.

There are, of course, many other graphs besides K -graphs which are free of two-line loops and hence have no logarithms in their imaginary part. In Appendix E we invoke a far-reaching combinatorial result of Bender and Canfield[18] which accounts for all such graphs. Despite its generality, however, the Bender and Canfield result does not immediately lend itself to an intuitive interpretation. For this reason we choose to illustrate many of our arguments by using the less comprehensive class of K -graphs. Though K -graphs represent the simplest generalization of multiperipheral graphs, our analysis is equally applicable to all logarithm-free graphs.

Before proceeding with our analysis of K -graphs, it is worthwhile mentioning how the extensively-studied factorial divergences[4, 7] in off-shell decay amplitudes $T_{1 \rightarrow \text{many}}$ fit into the present picture. Consider the graph of Fig. 6 in which two decay-like trees emerge from the point where p and p' meet. Summing over all such amplitudes and squaring yields a contribution to the total cross section and consequently also to $Im\ T_{2 \rightarrow 2}$. Suppose the tree-like decays in Fig. 6 terminate with the production of N_1 and N_2 particles where $N_1 + N_2 = N$. Assuming the equipartition of the center of mass energy E among all N particles, the sum over all Cayley tree graphs of the form of Fig. 6 results in a lower-bound contribution to $T_{2 \rightarrow N}$

$$T_{2 \rightarrow N} \doteq \sum_{N_1 + N_2 = N} F_{N_1} F_{N_2} \frac{N!}{N_1! N_2!}, \quad (5)$$

where[4]

$$F_{N_i} \doteq \left(\frac{g}{6\alpha^2} \right)^{N_i/2} N_i! \left(\frac{E}{N} \right)^{1-N_i} \quad (6)$$

with $\alpha = 2.92$. For such graphs we estimate the contribution

$$Im\ T_{2 \rightarrow 2} \doteq |T_{2 \rightarrow N}|^2 \rho_N / N! \quad (7)$$

where massless relativistic phase space is

$$\rho_N \doteq \left(\frac{E}{4\pi} \right)^{2N-4} \frac{1}{(N!)^2}. \quad (8)$$

Putting everything together, the contribution to $Im\ T_{2 \rightarrow 2}$ from Cayley trees is

$$Im\ T_{2 \rightarrow 2} \doteq N! \left(\frac{a_C g}{16\pi^2} \right)^N, \quad a_C = \frac{e^2}{6\alpha^2} \simeq 0.14 \quad . \quad (9)$$

Though Eq. 9 certainly implies factorially divergent behavior, it turns out we will obtain much stronger bounds on a from K -graphs ($a_K \geq 1/2$) and ultimately, in Appendix E, when we consider all logarithm-free graphs, we will bound $a \geq 2/3$ and estimate $a \simeq 0.94$.

2.2 Feynman-Parameter Representation of Graphs

This is a well-known subject[19], and we will be brief. Every graph we consider has just one UV logarithm in the real part, so the momentum integral must be regulated. This can be done with dimensional regularization or by applying $\partial/\partial m^2$ to the graph before performing the momentum integrals and then integrating with respect to m^2 after taking the imaginary part. Either way one finds that a N^{th} order graph (for N even) with symmetry factor S contributes

$$\text{Im } T_{2 \rightarrow 2} = \frac{g^2}{16\pi} \left(\frac{g}{16\pi^2} \right)^{N-2} \frac{1}{S} \int_0^1 \frac{[dx]}{U^2} \Theta\left(\frac{\phi}{U} - m^2\right), \quad (10)$$

where $[dx]$ is the usual measure associated with an integral over $2N - 2$ positive Feynman parameters x_i ,

$$[dx] = dx_1 \cdots dx_{2N-2} \delta\left(1 - \sum x_i\right). \quad (11)$$

U is the sum of all products of $N - 1$ Feynman parameters such that cutting the corresponding lines leaves a single connected tree graph. ϕ is given by

$$\phi = s\phi_s + u\phi_u \quad (12)$$

where ϕ_s (ϕ_u) is the sum of all products of N Feynman parameters such that cutting the corresponding lines splits the original graph into two connected trees with the square of the four-momentum entering each tree being $s = (p + p')^2$, ($u = (p - p')^2$). In general, ϕ also contains terms proportional to t and m^2 but these may be ignored because we are interested in forward scattering ($t = 0$) in the high-energy limit ($s \gg m^2$).

A crucial property of U is that it cannot vanish unless all of the parameters of a single loop vanish simultaneously. Consider a l -line loop labelled by the parameters x_1, x_2, \dots, x_l . Inserting in Eq. 10 the identity

$$1 = \int_0^1 d\lambda \delta\left(\lambda - \sum_1^l x_i\right) \quad (13)$$

and then performing the change of variables

$$x_i = \lambda \tilde{x}_i, \quad i = 1, \dots, l, \quad (14)$$

one finds that U vanishes linearly in λ as $\lambda \rightarrow 0$. If the Feynman parameters of another (possibly overlapping) loop are analogously scaled with a parameter λ' , then $U \sim \lambda\lambda'$ as $\lambda, \lambda' \rightarrow 0$. Since $U^2 \sim \lambda^2$ when λ is small, the λ -integral in Eq. 10 is of the form $\int_0^1 \lambda^{l-3} d\lambda$ which gives logarithms only if $l = 2$. Consequently, requiring an absence of two-line loops in a graph ensures an absence of logarithms in the contribution to $Im\ T_{2 \rightarrow 2}$.

2.3 K -graphs

Here we establish several properties of K -graphs, culminating in a lower bound on the contribution of all N^{th} order K -graphs to $Im\ T_{2 \rightarrow 2}$ which is indeed $O(N!)$. Our bound is of the form that the naive Lipatov analysis would give, although strictly speaking Lipatov's methods are not applicable for high-energy Minkowski-space graphs.

We begin by counting the number of N^{th} order K -graphs. Consider again the construction of two vertical lines or "walls" each of which has $N/2$ vertices; in a $2 \rightarrow 2$ multiperipheral amplitude these walls would correspond to the spacelike propagators: incoming momenta would be attached to the top and bottom of one wall while the outgoing momenta are similarly attached to the other wall. The remaining internal lines of a K -graph may then be visualized as the trajectory of a fictitious particle which "bounces" from wall to wall such that each of the N vertices is visited exactly once before the trajectory closes — this ansatz guarantees the absence of two-line loops.

Finding the number of possible trajectories in the above construction is a simple combinatoric exercise. Consider a trajectory as it leaves, say, the bottom vertex of the left wall: there are $\frac{N}{2}$ possible vertices on the right wall which the trajectory can intersect. After bouncing off the right wall, the trajectory can return to any one of $\frac{N}{2} - 1$ unvisited vertices on the left wall. Similarly, after bouncing off the left wall, there are $\frac{N}{2} - 1$ unvisited vertices on the right wall. Continuing in this manner, one finds exactly $(\frac{N}{2})!(\frac{N}{2} - 1)!$ possible directed trajectories. Dividing this number by two (to avoid double counting trajectories which are identical except for the sense in which they are traversed) we find that the number of N^{th} order K -graphs is

$$\frac{1}{2} \left(\frac{N}{2}\right)! \left(\frac{N}{2} - 1\right)! \doteq \frac{N!}{2^N} \quad (15)$$

where, as before, \doteq means equality modulo constant factors and fixed powers of N .

A consistent application of the Feynman rules demands that a sum of contributions to $Im\ T_{2 \rightarrow 2}$ of the form of Eq. 10 must include only topologically inequivalent graphs. It turns out, however, that not all $\frac{1}{2}(\frac{N}{2})!(\frac{N}{2} - 1)!$ K -graphs are topologically distinct: the first sign

of redundancy appears at $N = 10$ where the topologies of 12 graphs (out of 1440) appear twice. Fortunately, this level of duplication is insignificant (in the \doteq sense) and so we are still justified in identifying $N!/2^N$ in Eq. 15 as the number of topologically inequivalent K -graphs. Another minor point concerns the symmetry factor S associated with each K -graph in Eq. 10. Since the fraction of N^{th} order K -graphs with $S \neq 1$ goes to zero as N grows asymptotically large[20] we will implicitly assume that all K -graphs have $S = 1$.

We next direct our attention to the integral of Eq. 10. Using Eq. 12 and setting $u = -s$, the Θ -function appropriate for a K -graph is

$$\Theta\left(\frac{\phi_s - \phi_u}{U} - \frac{m^2}{s}\right) \simeq \Theta(\phi_s - \phi_u) \quad (16)$$

where we have legitimately dropped the small parameter $m^2/s \ll 1$ because there are no logarithmic divergences to regulate. Though the Θ -function in Eq. 10 poses no problem in principle, it can be eliminated if we consider additional contributions to $Im\ T_{2\rightarrow 2}$ which are closely related to those of K -graphs. To illustrate this point consider the K -graph of Fig. 3a and its associated u -channel exchange graph of Fig. 3b which is identical except for switching the vertices to which the ingoing and outgoing four-momentum vectors p' are attached. If the internal lines of Figs. 3a,b are labelled with the same Feynman parameters then it follows from the graph-based definition of U and ϕ that

$$U^{\text{Fig. 3b}} = U^{\text{Fig. 3a}}, \quad \phi_s^{\text{Fig. 3b}} = \phi_u^{\text{Fig. 3a}}, \quad \phi_u^{\text{Fig. 3b}} = \phi_s^{\text{Fig. 3a}}. \quad (17)$$

In other words, the Θ -functions associated with Figs. 3a,b sum to unity so that the corresponding joint contribution to $Im\ T_{2\rightarrow 2}$ is

$$Im\ T_{2\rightarrow 2} = \frac{g^2}{16\pi} \left(\frac{g}{16\pi^2}\right)^{N-2} \int_0^1 \frac{[dx]}{U^2}. \quad (18)$$

It is clear that the Θ -function for any K -graph can similarly be eliminated by including the appropriate u -channel exchange graph. Over-counting is not an issue for the graphs of Figs. 3a,b. When Fig. 3b is redrawn in Fig. 3c it is apparent that it is not one of the original $\frac{1}{2}(\frac{N}{2})!(\frac{N}{2} - 1)!$ K -graphs. There are, however, a small number (in the \doteq sense) of K -graphs whose exchange graphs are themselves K -graphs. Though such graphs pose no problem in principle, we will neglect them in order to keep our discussion simple.

If we implicitly agree to include u -channel exchange graphs, all that remains is to evaluate

$$I_i = \int_0^1 \frac{[dx]}{U_i^2} \quad (19)$$

where U_i is the U function for i^{th} K -graph and then to sum over all $N!/2^N$ K -graphs. As far as we know it is impossible to calculate I_i analytically but one can obtain useful lower bounds from the following simple considerations. For each graph we define the normalized probability density p_i for U ,

$$p_i = \frac{\int_0^1 [dx] \delta(U - U_i(x))}{\int_0^1 [dx]}. \quad (20)$$

It is not difficult to show that $\int_0^1 [dx] = 1/(2N-3)!$ which allows us to write

$$\begin{aligned} I_i &= \frac{1}{(2N-3)!} \int dU \frac{p_i}{U^2} \\ &\equiv \frac{1}{(2N-3)!} \left\langle \frac{1}{U^2} \right\rangle_i \\ &\geq \frac{1}{(2N-3)!} \frac{1}{\langle U \rangle_i^2}, \end{aligned} \quad (21)$$

where $\langle 1/U^2 \rangle_i \geq 1/\langle U \rangle_i^2$ follows from the Hölder inequality[21]

$$\int dU f g \geq \left(\int dU f^k \right)^{1/k} \left(\int dU g^{k'} \right)^{1/k'} \quad (22)$$

with $f = U/\sqrt{p_i}$, $g = (p_i)^{3/2}$, $k = -2$ and $k' = k/(k-1) = 2/3$.

Our interest in the bound of Eq. 21 arises from the fact that $\langle U \rangle_i$ is easily calculated for any given graph. Specifically, one has

$$\langle U \rangle_i = C_i (2N-3)! \int_0^1 [dx] x_1 x_2 \cdots x_{N-1}, \quad (23)$$

where C_i is the number of terms in U_i . In graph-theoretic language C_i is known as the complexity or number of spanning trees of a graph[22]. The integral in Eq. 23 is elementary; starting from the Feynman identity

$$\prod_{i=1}^{2N-2} \frac{1}{A_i} = (2N-3)! \int [dx] \left(\sum A_i x_i \right)^{2N-2} \quad (24)$$

and differentiating once with respect to A_1, A_2, \dots, A_{N-1} and then setting all the $A_i = 1$, one finds $\int_0^1 [dx] x_1 x_2 \cdots x_{N-1} = 1/(3N-4)!$. Summing over all N^{th} order K -graphs, we obtain the bound

$$\sum_i I_i \geq \frac{(3N-4)!^2}{(2N-3)!^3} \sum_i \frac{1}{C_i^2}. \quad (25)$$

We next introduce a normalized complexity density function

$$p_C \equiv \frac{2^N}{N!} \sum_i \delta(C - C_i) \quad (26)$$

where again the sum is over all N^{th} order K -graphs. In this language we have

$$\sum_i I_i \geq \frac{(3N-4)!^2}{(2N-3)!^3} \frac{N!}{2^N} \left\langle \frac{1}{C^2} \right\rangle \quad (27)$$

where

$$\left\langle \frac{1}{C^2} \right\rangle \equiv \int dC \frac{p_c}{C^2} . \quad (28)$$

Using the Hölder inequality to show that $\langle 1/C^2 \rangle \geq 1/\langle C \rangle^2$, one has

$$\sum_i I_i \geq \frac{(3N-4)!^2}{(2N-3)!^3} \frac{N!}{2^N} \frac{1}{\langle C \rangle^2} . \quad (29)$$

We have studied the complexity density functions of K -graphs up to $N = 400$ and we find (see Appendix A) the empirical asymptotic relation

$$\langle C \rangle \simeq \frac{.56}{N} \left(\frac{27}{8} \right)^N \quad (30)$$

which works to better than $\simeq 5\%$ for $N \geq 20$. (In the range $20 \leq N \leq 400$, $\langle C \rangle$ varies by 200 orders of magnitude, so this is a very accurate fit for the constant $27/8$ in Eq. 30.) Using Eq. 30 in Eq. 29 we find, for $N \gg 1$,

$$\sum_i I_i \geq \frac{1}{(.56)^2} \left(\frac{2}{3} \right)^7 \frac{N^2}{\sqrt{2}} \left(\frac{1}{2} \right)^N N! \doteq \left(\frac{1}{2} \right)^N N! \quad (31)$$

In other words, the contribution of all N^{th} order K -graphs to $Im T_{2 \rightarrow 2}$ is

$$Im T_{2 \rightarrow 2} \doteq N! \left(\frac{a_K g}{16\pi^2} \right)^N , \quad (32)$$

where $a_K \geq 1/2$. If one includes all $g\phi^4$ graphs without two-line loops, the corresponding limit is $a \geq 2/3$ (see Appendix E). These bounds may also be derived without using the complexity results of Eq. 30 by instead bounding the asymptotic behavior of the integrals $\int [dx]/U_i^2 \geq \int [dx]/U_S^2$ where U_S is the completely symmetric sum of products of $N-1$ Feynman parameters (see Appendix B). In Appendix B we also use integrals of U_S to speculate upon possible improvements to the bounds on a . These speculations amount to multiplying a_K by the ratio $C_S^2/\langle C \rangle^2$, where $C_S \doteq 4^N$ is the complexity of U_S ; this leads to estimating $a_K \geq 512/729 \simeq 0.7$ if one includes only K -graphs and $a \geq 2048/2187 \simeq 0.94$ if one includes all simple graphs as in Appendix E. Presumably the answer for the sum of all graphs without logarithms is Eq. 32 with $a = 1$, the Lipatov result. Though K -graphs are fundamentally rooted in Minkowski space at large momenta they have much in common with graphs having no external momenta, as required by the Lipatov technique. In Appendix C we point out striking statistical regularities which arise in the integrals of the U_i .

3 Summing K –Graphs and Two-Line Loops

In this section we investigate the marriage of the factorial behavior of K –graphs with leading logarithmic behavior in $g\phi^4$ theory. Specifically, we sum contributions to $Im\ T_{2\rightarrow 2}$ from chain graphs of the form shown in Fig. 7 which are constructed by joining arbitrary combinations of K –graphs and two-line loops. The sum of all such graphs and their u –channel exchange graphs is summarized by the Bethe-Salpeter equation depicted in Fig. 8.

A key result which makes summing all chain graphs feasible is a factorization theorem illustrated by Fig. 9; we prove the theorem in Appendix D. The essence of the theorem is that, up to leading logarithms, one may factor a K –graph from a graph and replace it with a two-line loop. The constant of proportionality between the imaginary parts of the two graphs is

$$\hat{K} = \frac{(Im\ T_{2\rightarrow 2})_K}{(Im\ T_{2\rightarrow 2})_{N=2}} = 2 \left(\frac{g}{16\pi^2} \right)^{N_K-2} \int_0^1 \frac{[dx]}{U_K^2} , \quad (33)$$

where $(Im\ T_{2\rightarrow 2})_K$ is the contribution to $Im\ T_{2\rightarrow 2}$ from the corresponding isolated N_K^{th} order K –graph and its u –channel exchange graph (e.g., as in Fig. 8d,e) and $(Im\ T_{2\rightarrow 2})_{N=2}$ is the contribution from a single two line loop (e.g., as in Fig. 8b,c).

The ability to factor K –graphs out of chain graphs effectively reduces the problem of solving the Bethe-Salpeter equation of Fig. 8 to the much simpler and well-studied [10, 11] problem of summing ladder graphs. Denoting terms in the Bethe-Salpeter equation by their labels in Fig. 8, one has from Fig. 9 and Eq. 33,

$$(Im\ T_{2\rightarrow 2})_b + (Im\ T_{2\rightarrow 2})_c = (Im\ T_{2\rightarrow 2})_{N=2} , \quad (34)$$

$$(Im\ T_{2\rightarrow 2})_d + (Im\ T_{2\rightarrow 2})_e = \left(\sum \hat{K}_i \right) (Im\ T_{2\rightarrow 2})_{N=2} , \quad (35)$$

$$(Im\ T_{2\rightarrow 2})_f + (Im\ T_{2\rightarrow 2})_g = \left(1 + \sum \hat{K}_i \right) (Im\ T_{2\rightarrow 2})_f , \quad (36)$$

so that the Bethe-Salpeter of Fig. 8 becomes

$$(Im\ T_{2\rightarrow 2})_a = \left(1 + \sum \hat{K}_i \right) [(Im\ T_{2\rightarrow 2})_{N=2} + (Im\ T_{2\rightarrow 2})_f] . \quad (37)$$

The terms in square brackets of Eq. 37 are recognized as the right hand side of the Bethe-Salpeter equation appropriate for summing straight ladders. Consequently, the Bethe-Salpeter equation involving K –graphs is solved by taking the solution to the corresponding sum of ladder graphs (Eq. 1) and making the substitution

$$g \rightarrow g \left(1 + \sum \hat{K}_i \right)^{1/2} . \quad (38)$$

With the substitution of Eq. 38 we obtain

$$Im T_{2 \rightarrow 2}(s \gg m^2, t = 0) \sim \frac{g^2 (1 + \sum \hat{K}_i)}{\ln^{3/2}(s/m^2)} \left[\left(\frac{s}{m^2} \right)^{\frac{g}{16\pi^2} (1 + \sum \hat{K}_i)^{1/2}} + (g \rightarrow -g) \right] \quad (39)$$

where, from section 2.3,

$$\sum \hat{K}_i \doteq \sum_{\text{even } N} N! \left(\frac{ag}{16\pi^2} \right)^N. \quad (40)$$

Naturally, Eq. 38 can also be deduced by considering the effect of the factorization theorem on individual chain graphs like Fig. 7. Consider the set of chain graphs with $N/2$ “rungs” where a rung is either a K –graph or a two-line loop. By the factorization theorem, the sum of all such chains is proportional to the N^{th} order uncrossed ladder graph (where all rungs are two-line loops) and the factor of proportionality follows by summing over the possible replacements of two-line loops with K –graphs. Let n_i denote the number of times a K_i –graph appears in the chain. The factorization theorem and elementary combinatorics give the overall factor of proportionality

$$\sum_{\{n_i\}} \frac{(N/2)!}{n_{i_1}! n_{i_2}! \cdots (N/2 - \sum_i n_i)!} \prod_i \hat{K}_i^{n_i}, \quad (41)$$

where the sum over n_i is such that $\sum_i n_i \leq N/2$. Eq. 41 is simply the multinomial expansion of $(1 + \sum \hat{K}_i)^{N/2}$ so that summing over all insertions of K –graphs is equivalent to the ladder graph result with the substitution of Eq. 38.

4 Conclusions

By summing graphs in $g\phi^4$ theory, we have shown how a Regge-like energy behavior and a Lipatov-like $N!g^N$ behavior co-exist at high energies. The Lipatov analysis is restricted to zero four-momentum, and fails to be directly applicable to overall high-energy process. But we have found classes of graphs (like K –graphs) which very much resemble zero-momentum graphs and which give various hints of being amenable to semi-classical analysis. These graphs factor out of energy-dependent processes and can be analyzed separately. Presently we do not know how to calculate sets of graphs like K –graphs with semi-classical techniques, but there surely must be such a method which might ultimately tell us how to factor all relevant graphs out of high-energy processes and how to calculate the coefficient a in the expansion $N! \left(\frac{ag}{16\pi^2} \right)^2$ without approximation. (Of course, we expect to find the Lipatov value $a = 1$).

Many other issues remain unsettled. For example, our graphical analysis occurred in the absence of derivative couplings and involved the dimensionless quantities g and $Im\ T_{2\rightarrow 2}$; these are the circumstances under which one also expects to succeed with a Lipatov analysis. But in realistic theories like QCD, and even in $g\phi^4$ (e.g., if studying $T_{2\rightarrow N}$) one or all of these conditions is not met.

Consider, for example, the amplitude $T_{2\rightarrow N}$ in $g\phi^4$ theory. The very special case where all but two of the final-state particles have zero four-momentum can be obtained from our previous results. In the basic graph of Fig. 2 from which all our other graphs are derived, let the masses of the left-hand vertical lines be M_1 and that of the right-hand lines be M_2 ; roughly speaking, this replaces m^2 in $\ln(s/m^2)$ by $\frac{1}{2}(M_1^2 + M_2^2)$. Applying $g\frac{\partial}{\partial M_2^2}$ N times to $Im\ T_{2\rightarrow 2}$ produces a contribution to $Im\ T_{2\rightarrow 2N+2}$ whose energy dependence is unchanged from that of $Im\ T_{2\rightarrow 2}$; it has simply picked up a factor of M_2^{-2N} . Yet when the $2N$ added particles all have large momenta, of order $\frac{\sqrt{s}}{2N}$, we expect an energy dependence where M_2^{-2N} is replaced by s^{-N} . This regime, when many particles have large energy, simply cannot be addressed in any straightforward way by Lipatov techniques. The difficulty also shows up in the graphical analysis where the relatively simple integrals for K -graphs such as Eq. 10 are replaced by integrals which involve powers of the energy-dependent function ϕ . Even more drastic changes occur for QCD where, because of derivative couplings, not only do powers of ϕ appear but altogether different combinations of Feynman parameters arise[23].

There is another stumbling block on the road to QCD. At high energy, with $s \gg |t|$, it is well-known[24] that QCD Reggizes somewhat as ϕ^4 theory does, but the equivalent of the K -graphs are not four-dimensional Feynman graphs, as in ϕ^4 theory, but two-dimensional, referring only to momentum transverse to p and p' . The underlying two-dimensional theory is presumably a sigma model, as the Verlinde[15] have suggested, but the usual Lipatov analysis has not been applied here.

We do, however, know something about leading-logarithm behavior in QCD when $s \gg t \gg m^2$ [24] where m^2 is either a fictitious mass or a Higgs mass for the gauge boson[26]. The analog of Eq. 1 for non-forward scattering in QCD yields amplitudes which vary as $s^{\alpha_P(t)}$ where the ‘‘Pomeron’’ trajectory α_P is given by, to $O(\alpha_S)$ in the strong coupling constant α_S ,

$$\alpha_P(|t| \gg m^2) = 1 - \frac{\alpha_S N_C}{2\pi} \ln \left(\frac{|t|}{m^2} \right), \quad (42)$$

where N_C is the number of colors. Suppose, for the sake of argument, that including the

QCD analog of K -graphs leads to the replacement

$$\alpha_S \rightarrow \alpha_S \left(1 + \sum_N \left[-\frac{\alpha_S N_C}{2\pi} \ln \left(\frac{|t|}{m^2} \right) \right]^N N! \right). \quad (43)$$

Eq. 43 corresponds to Eq. 2 except that now there is a t -dependence due to non-forward scattering. At this point, only leading IR logs have been kept but it is possible to renormalization group (RG) improve Eq. 42 (and, correspondingly Eq. 43) and incorporate the effects of the one-loop running charge

$$\bar{\alpha}_S(t) = \frac{1}{4\pi b \ln(|t|/m^2)}, \quad b = \frac{1}{48\pi^2}(11N_C - 2N_F), \quad (44)$$

where N_F is the number of flavors. The RG-improved result is not quite the naive result of replacing α_S by $\bar{\alpha}_S$ [25] but rather, Eq. 43 becomes

$$\bar{\alpha}_S \rightarrow \bar{\alpha}_S \left(1 + \sum_N \gamma^N(t) N! \right), \quad \gamma(t) = \frac{6N_C}{11N_C - 2N_F} \ln \left(\ln \left(\frac{|t|}{m^2} \right) \right). \quad (45)$$

Previous experience[26] with unitarizing factorially divergent series such as Eq. 45 suggests that the largest value of N which can be trusted is $N = 1/\gamma$, but this is typically not even as large as 2. QCD perturbation theory for high-energy fixed- t processes is subject to large effects from $N!$ divergences even for small N . This is not what one might have guessed by looking at the kind of series one gets just from the Lipatov analysis, which applies to purely s -wave processes and looks something like

$$\sum_N \left(\frac{\alpha_S}{2\pi} \right)^N N! \quad \text{or} \quad \sum_N \left(\frac{\bar{\alpha}_S}{2\pi} \right)^N N! \quad (46)$$

The second form is, of course, RG-improved, with the argument of $\bar{\alpha}_S$ now being s , not t . The RG-improved series begins to diverge at $N \simeq \frac{1}{2}(11N_C - 2N_F) \ln(s/m^2)$ which typically is considerably larger than one.

5 Acknowledgements

JMC is supported by the National Science Foundation under grant PHY-9218990. We would like to thank D. Cangemi and S. Nussinov for many discussions.

A Complexity of K –Graphs

In this appendix we present results on the distribution of complexity of K –graphs. A useful result from algebraic graph theory is an expression for the complexity of an N^{th} order graph[22, 27],

$$C = \frac{\det(J + Q)}{N^2}, \quad (47)$$

where J is an $N \times N$ matrix whose matrix elements are all equal to unity, and Q is a $N \times N$ symmetric matrix. For $2 \rightarrow 2$ graphs in $g\phi^4$ theory, Q may be constructed as follows. Draw an N^{th} order graph with its external lines truncated and label the vertices from 1 to N . The diagonal matrix elements Q_{ii} are the number of lines attached to the i^{th} vertex. The off diagonal matrix elements are such that $-Q_{ij}$ is the number of lines joining vertex i to vertex j .

Figure 10 shows the distribution of complexities for all 43,200 K –graphs for $N = 12$. Table 1 lists the average complexity of K –graphs for various orders of perturbation theory. A least-squares fit of $\langle C \rangle$ over $20 \leq N \leq 400$ to the form $c_1 N^{c_2} c_3^N$ (with c_2 an integer) yields the best fit

$$\langle C \rangle \simeq \frac{.5585}{N} (3.3752)^N, \quad (48)$$

which is accurate to better than 0.5% (comparable to the accuracy with which the actual averages are determined). In fact, using $\langle C \rangle \simeq \frac{.5585}{N} (27/8)^N$ works better than 5% which is impressive since $\langle C \rangle$ varies by 200 orders of magnitude over the range in question. Though we have not pursued an analytic calculation of $\langle C \rangle$ for K –graphs, it not unreasonable to believe that such an approach exists for asymptotically large N since analogous graph-theoretic problems have been encountered previously in the study of cluster integrals in statistical mechanics[27]. The near-Gaussian nature of the complexity distribution and the N –dependence of $\langle C \rangle$ are analogous to the observations of Bender and Wu[16] concerning the behavior of connected vacuum diagrams in ϕ^4 theory in one spacetime dimension.

B Bounds From Completely Symmetric U_S

The functions U_i characterizing contributions of N^{th} order K –graphs to $Im T_{2 \rightarrow 2}$ share the feature that they are sums of monomials formed from the products of $N - 1$ Feynman parameters (out of a possible $2N - 2$ parameters). Since the number of monomials in U_i (that is, the complexity C_i) varies from graph to graph it is in practice difficult, if not impossible, to obtain analytic expressions for integrals of the form $\int [dx]/U_i^2$. However, one can hope

to evaluate integrals of the completely symmetric function U_S which, at N^{th} order, is the symmetric sum of all possible combinations of products of $N - 1$ parameters chosen from $2N - 2$ parameters. Since $U_S \geq U_i$, one obtains the bound $\int_0^1 [dx]/U_i^2 \geq \int_0^1 [dx]/U_S^2$.

In this appendix we investigate the large- N behavior of the integral

$$I_S(2N - 2) \equiv \int_0^1 \frac{[dx]}{U_S^2}, \quad [dx] = dx_1 dx_2 \cdots dx_{2N-2} \delta\left(1 - \sum_j^{2N-2} x_j\right) \quad (49)$$

and we use our results to place lower bounds on the corresponding integrals of the U_i functions. To our knowledge $I_S(2N - 2)$ cannot be performed directly so instead, letting $n = 2N - 2$, we concentrate on

$$I_S(n \gg 1, k) \equiv \int [dx] U_S^k \quad (50)$$

for non-negative integer k with the intention of analytically continuing to $k = -2$. In Sect. B.1 we find that, to leading order in n ,

$$I_S(n \gg 1, k) \simeq \frac{(2\pi n)^{-k/2}}{\Gamma\left(n\left(\frac{k}{2} + 1\right)\right)} \left(\frac{2z^{-k/2}}{2 - kz}\right)^n \sqrt{\left(\frac{2z(1 - k)}{z - 1}\right)^{k-1} \frac{4z}{z(k + 2) - 2}}, \quad (51)$$

where z is a function of k given implicitly by

$$\frac{d}{dz} \left(z^{k/2} e^{1/z} \Gamma(k + 1, 1/z) \right) = 0, \quad (52)$$

where $\Gamma(k + 1, 1/z) = \int_{1/z}^{\infty} dt e^{-t} t^k$ is the incomplete gamma function.

In Sect. B.2 we demonstrate that Eq. 51 yields impressive agreement with numerical integration of $I_S(n, k)$ for $k \gtrsim -2$ but becomes unreliable very close to $k = -2$ (when $|k + 2| \lesssim O(1/n)$). Nevertheless, we argue that the large- n behavior of $I_S(n, k = -2)$ is already contained in Eq. 51 and that, modulo an overall constant and a fixed power of n , $I_S(n \gg 1, k = -2) \doteq 1$.

In Sect. B.3 we demonstrate how the bound $Im T_{2 \rightarrow 2} \doteq N! \left(\frac{ag}{16\pi^2}\right)^N$ with $a_K \geq 1/2$ follows from a consideration of symmetric functions. In addition, we speculate about upon possible improvements to which may make $a_K \simeq 0.7$. Analogous reasoning is applied to the set of all simple graphs (of which K -graphs are a subset) in Appendix E.

B.1 Saddle Point Evaluation of $I(n \gg 1, k)$

For non-negative integer k one can expand U_S^k and integrate term by term to get

$$I_S(n, k) = \frac{n!}{(n + kn/2 - 1)!} \sum_{\{n_j^{(q)}\}} \left(\prod_{j,(q)} \frac{(j!)^{n_j^{(q)}}}{n_j^{(q)}!} \right), \quad (53)$$

where the sum over the non-negative integer variables $\{n_j^{(q)}\}$ is subject to the $k+1$ constraints

$$\sum_{j=0}^{j=k} \sum_{(q)} n_j^{(q)} = n, \quad \sum_{j=1}^{j=k} \sum_{(mq)} n_j^{(mq)} = \frac{n}{2} \quad \text{for } m = 1, \dots, k. \quad (54)$$

We will not discuss the motivation for introducing the $\{n_j^{(q)}\}$ except to point out that they arise naturally from a combinatoric analysis of terms in the expansion of U_S^k . Our notation for $n_j^{(q)}$ is such that (q) is a combination of j integers chosen from 1 to k . For example, for $k = 3$ the relevant set of variables is $\{n_0^{(0)}, n_1^{(1)}, n_1^{(2)}, n_1^{(3)}, n_2^{(12)}, n_2^{(13)}, n_2^{(23)}, n_3^{(123)}\}$; in general there are 2^k different $n_j^{(q)}$. The label (mq) in $n_j^{(mq)}$ denotes a combination of j integers which includes the integer m .

To find $I_S(n \gg 1, k)$ we replace the discrete sum in Eq. 53 with an integral of the corresponding continuous quantity

$$I_S(n \gg 1, k) \simeq \frac{\Gamma(n+1)}{\Gamma\left(n\left(\frac{k}{2}+1\right)\right)} \int \prod_{j,(q)} \frac{dn_j^{(q)} (j!)^{n_j^{(q)}}}{\Gamma(n_j^{(q)}+1)} \prod_{m=0}^{m=k} \frac{d\lambda_m}{2\pi} e^{i\lambda_m f_m}, \quad (55)$$

where the constraints have been incorporated by defining

$$f_0 = n - \sum_{j=0}^{j=k} \sum_{(q)} n_j^{(q)}, \quad f_m = \frac{n}{2} - \sum_{j=1}^{j=k} \sum_{(mq)} n_j^{(mq)}, \quad \text{for } m = 1, \dots, k. \quad (56)$$

With the approximation $\Gamma(p+1) \simeq \sqrt{2\pi p} (p/e)^p$ we can rewrite Eq. 55 in the form

$$I_S(n \gg 1, k) \simeq \frac{\Gamma(n+1)}{\Gamma\left(n\left(\frac{k}{2}+1\right)\right) (2\pi)^{(k+1+2^{k-1})}} \int \prod_{j,(q)} dn_j^{(q)} \prod_{m=0}^{m=k} d\lambda_m e^F, \quad (57)$$

where the argument of the exponential is

$$F = \sum_{j=0}^{j=k} \sum_{(q)} \left(n_j^{(q)} \ln j! - (n_j^{(q)} + \frac{1}{2}) \ln n_j^{(q)} + n_j^{(q)} \right) + i \sum_{j=0}^{j=k} \lambda_j f_j. \quad (58)$$

Using Laplace's method to evaluate $I_S(n \gg 1, k)$ we find that the extremum of F occurs when $n_j^{(q)} = \bar{n}_j \equiv j! x z^j$ where $z \equiv e^{i\bar{\lambda}}$, $x \equiv e^{i\bar{\lambda}_0}$ and overbars denote parameter values at the extremum.

At the extremum, $f_0 = f_m = 0$ so that the constraints of Eq. 56 become

$$x \sum_{j=0}^{j=k} \binom{k}{j} j! z^j = n, \quad x \sum_{j=1}^{j=k} \binom{k-1}{j-1} j! z^j = \frac{n}{2}, \quad (59)$$

which may be rewritten as

$$\frac{d}{dz} \left(z^{k/2} e^{1/z} \Gamma(k+1, 1/z) \right) = 0, \quad x = \frac{n}{2} (2 - kz). \quad (60)$$

We can proceed to perform the integrations in Eq. 57 by expanding F around its maximum

$$F = F|_{\bar{y}} + \sum_{i,j=1}^{2^k+k+1} \frac{1}{2} \frac{\partial^2 F}{\partial y_i \partial y_j} \Big|_{\bar{y}} (y_i - \bar{y}_i)(y_j - \bar{y}_j) + \dots \quad (61)$$

where the first 2^k of the y_i variables are the $n_j^{(q)}$ and the remaining $k+1$ variables are $i\lambda_j$ for $(j = 0, \dots, k)$. Performing the Gaussian integrations we obtain

$$I_S(n \gg 1, k) \simeq \frac{(2\pi)^{-k/2}}{\Gamma\left(n\left(\frac{k}{2} + 1\right)\right)} \left(\frac{2z^{-k/2}}{2 - kz}\right)^n \sqrt{\frac{n}{\det(A)} \prod_{j(q)} \frac{1}{\bar{n}_j^{(q)}}}. \quad (62)$$

where A is the matrix defined by

$$A_{ij} = - \frac{\partial^2 F}{\partial y_i \partial y_j} \Big|_{\bar{y}}. \quad (63)$$

After a somewhat lengthy but straightforward manipulation, $\det(A)$ can be written as

$$\det(A) = (-n)^{k+1} \frac{2z + kz - 2}{4z} \left(\frac{z-1}{2z(1-k)}\right)^{k-1} \prod_{j(q)} \frac{1}{\bar{n}_j^{(q)}}, \quad (64)$$

which, when substituted in Eq. 62 gives the result of Eq. 51.

B.2 The Limit $k \rightarrow -2$

We have compared $I_S(n \gg 1, k)$ of Eq. 51 with results from integrating $\int [dx] U_S^k$ numerically for $n \leq 20$. As can be seen from Fig. 11, where we show the comparison for $n = 20$, the analytic continuation of Eq. 51 to negative k is successful (agreeing up to a correction

factor of $1 + O(1/n)$ until $k \simeq -2$. The nature of the discrepancy is made evident by noting that as $k \rightarrow -2$, Eq. 52 reduces to the asymptotic relation

$$k + 2 \simeq \frac{2 \ln z}{z} , \quad (65)$$

As $k \rightarrow 2$, Eq. 51 becomes

$$I_S(n \gg 1, k \simeq -2) \simeq \frac{\pi n^2}{3\sqrt{6}} \sqrt{k+2}. \quad (66)$$

which suggests that the neglected corrections are such that

$$I_S(n \gg 1, k \simeq -2) \simeq \frac{\pi n^2}{3\sqrt{6}} \sqrt{k+2} \left[1 + O\left(\frac{1}{n\sqrt{k+2}}\right) \right]. \quad (67)$$

Indeed, numerical integration of $I_S(n, k = -2)$ for $6 \leq n \leq 20$ is consistent with $I_S(n, k = -2) \sim n$.

In any case, our goal is to extract the large- N behavior of $I_S(2N-2, k = -2)$. As has already been exploited in taking the $k \rightarrow -2$ limit of Eq. 51 to arrive at Eq. 66,

$$\lim_{k \rightarrow -2} \left(\frac{2z^{-k/2}}{2 - kz} \right)^n = 1^n , \quad (68)$$

since $z \rightarrow \infty$ as $k \rightarrow -2$. In other words, with the $O(1/N)$ corrections of Eq. 67 taken into account,

$$I_S(2N-2 \gg 1, k = -2) \doteq 1. \quad (69)$$

B.3 Bounds on $Im \ T_{2 \rightarrow 2}$

Without making recourse to the complexity results of Appendix A one can reproduce the lower bound $a_K \geq 1/2$ for contributions to $Im \ T_{2 \rightarrow 2}$ simply by considering integrals of the completely symmetric functions U_S . Since $U_S \geq U_i$, it follows that the contributions of all N^{th} order K -graphs obey the bound

$$\begin{aligned} Im \ T_{2 \rightarrow 2} &= \frac{g^2}{16\pi} \left(\frac{g}{16\pi^2} \right)^{N-2} \sum_i \int \frac{[dx]}{U_i^2} \\ &\geq \frac{g^2}{16\pi} \left(\frac{g}{16\pi^2} \right)^{N-2} \sum_i \int \frac{[dx]}{U_S^2} \\ &\doteq \frac{N!}{2^N} \left(\frac{g}{16\pi^2} \right)^N \\ &= N! \left(\frac{ag}{16\pi^2} \right)^N \end{aligned} \quad (70)$$

with $a = 1/2$. In going from the second to third lines of Eq. 70, we have used the asymptotic behavior of Eq. 69 and summed over the number of N^{th} order K -graphs which is $\doteq N!/2^N$.

If we wish to be adventuresome we can contemplate extending the lower bounds on $Im\ T_{2\rightarrow 2}$ even further by combining the complexity results of Appendix A with the asymptotic behavior of the integrals of U_S . Letting $C_S = (2N - 2)!/(N - 1)!^2 \doteq 4^N$ denote the number of terms in U_S , it follows from Eq. 23 that

$$\frac{\langle U_i \rangle}{C_i} = \frac{\langle U_S \rangle}{C_S}, \quad (71)$$

where C_i is the complexity of U_i . Although Eq. 71 strictly only refers to the average values of U_S and U_i , it is amusing to explore the consequences of extending the relation $U_i \leq U_S$ by assuming that, in the region $U_i \simeq 0$ (where the important contributions to $\int [dx]/U_i^2$ arise),

$$\frac{U_i}{C_i} \lesssim \frac{U_S}{C_S}. \quad (72)$$

The motivation for this assumption is that when C_i becomes large, then for fixed values of the $2N - 2$ Feynman parameters $\{x_i\}$, U_i/C_i can be thought of as an estimate of the average value of all C_S possible monomials formed from combinations of $N - 1$ of the x_i ; the true average of these monomials (for the same fixed $\{x_i\}$) is, naturally, U_S/C_S . Of course, the monomials in U_i are not random — they arise from K -graphs. The assumption that U_i/C_i is smaller than U_S/C_S is an attempt to reflect the correlations among monomials in U_i make which it easy for U_i to be small: only 3 Feynman parameters (corresponding to three-line loops) need vanish simultaneously for U_i to vanish whereas $N - 1$ parameters must simultaneously vanish for U_S to go to zero.

Under the assumption of the inequality of Eq. 72 the contribution of all N^{th} order K -graphs is

$$\begin{aligned} Im\ T_{2\rightarrow 2} &= \frac{g^2}{16\pi} \left(\frac{g}{16\pi^2} \right)^{N-2} \sum_i \int \frac{[dx]}{U_i^2} \\ &\geq \frac{g^2}{16\pi} \left(\frac{g}{16\pi^2} \right)^{N-2} \sum_i \left(\frac{C_S}{C_i} \right)^2 \int \frac{[dx]}{U_S^2} \\ &\doteq \left(\frac{g}{16\pi^2} \right)^N \sum_i \left(\frac{4^N}{(27/8)^N} \right)^2 \\ &\doteq N! \left(\frac{a_K g}{16\pi^2} \right)^N \end{aligned} \quad (73)$$

with $a = 512/729 \simeq .70$ and where we have used the asymptotic behavior of I_S and the empirical average complexity of the K -graphs found in Appendix A. We emphasize that

the inequality of Eq. 72, though plausible, is only an assumption. It is consistent with our numerical work where limitations of computer time make checks feasible. It is plausible that the bound $a_K \geq 1/2$ or perhaps even $a_K \simeq 0.7$ could be sharpened with a judicious application of inequalities to the information already at hand.

C Regularity of Contributions To $Im\ T_{2 \rightarrow 2}$

In this appendix we present evidence for regularities in the contributions of N^{th} order K -graphs to $Im\ T_{2 \rightarrow 2}$. The sum of these contributions (including u -channel exchange graphs) is

$$Im\ T_{2 \rightarrow 2} = \frac{g^2}{16\pi} \left(\frac{g}{16\pi^2} \right)^{N-2} \sum_i \int_0^1 \frac{[dx]}{U_i^2}, \quad (74)$$

where U_i characterizes the i^{th} K -graph. In section 2.3 we defined for each graph the probability density p_i which treats U as an independent variable and we derived lower bounds for the integrals of Eq. 74 in terms of the expectation values $\langle U \rangle_i = \int dU p_i U$ (see Eq. 21). Whereas the distribution of the complexity C_i (see e.g., Fig. 10) reflects regularity in $\langle U \rangle_i$, we now wish to point out a strong correlation between the shapes of the probability densities p_i themselves.

To facilitate a comparison of the p_i , we first rescale from the variable U to the variable $\tilde{U} = U/\langle U \rangle_i$ so that $\langle \tilde{U} \rangle_i = 1$ for all K -graphs. In other words, it is convenient to compare the probability densities \tilde{p}_i defined by

$$\tilde{p}_i = \frac{\int_0^1 [dx] \delta\left(\tilde{U} - \frac{U_i(x)(3N-4)!}{C_i}\right)}{\int_0^1 [dx]}. \quad (75)$$

In terms of the \tilde{p}_i ,

$$\int_0^1 \frac{[dx]}{U_i^2} = \frac{(3N-4)!^2}{(2N-3)! C_i^2} \int d\tilde{U} \frac{\tilde{p}_i}{\tilde{U}^2}. \quad (76)$$

Figure 12 superimposes the results of Monte Carlo calculations of \tilde{p}_i for all 72 K -graphs at order $N = 8$. The striking degree of similarity between the various distributions makes plausible the existence of a single representative function \tilde{p} such that $\int d\tilde{U} \tilde{p}/\tilde{U}^2 \simeq \int d\tilde{U} \tilde{p}_i/\tilde{U}^2$ is independent of the graph under consideration. Limited information on \tilde{p} can be gleaned by looking at the moments of \tilde{p}_i . For relatively small values of N ($N = 6, 8$) we have calculated connected moments of \tilde{p}_i and find that these fall very rapidly compared to disconnected moments; this is evidence that \tilde{p} is quite Gaussian above some value which near is or below

$\tilde{U} = 1$. Not much can be learned about the small- \tilde{U} behavior of \tilde{p} from direct numerical calculation; all that we know for sure is that $\tilde{p} \simeq \tilde{U}^2$ when \tilde{U} is small, since by arguments like those given in connection with Eq. 14, the moments $\langle \tilde{U}^k \rangle$ of \tilde{p} exist for $k > -3$ and diverge at $k = -3$. Perhaps \tilde{p} is \tilde{U}^2 times a Gaussian. For comparison, the solid line of Fig. 12 shows the rescaled probability density corresponding to the completely symmetric U -function.

Summing over all K -graphs, we can use the hypothesized density \tilde{p} to write

$$\begin{aligned} \sum I_i &\simeq \frac{(3N-4)!^2}{(2N-3)!} \left(\int d\tilde{U} \frac{\tilde{p}}{\tilde{U}^2} \right) \sum_i \frac{1}{C_i^2} \\ &= \frac{(3N-4)!^2}{(2N-3)!} \frac{N!}{2^N} \left(\int d\tilde{U} \frac{\tilde{p}}{\tilde{U}^2} \right) \left\langle \frac{1}{C^2} \right\rangle. \end{aligned} \quad (77)$$

In other words, the contributions of K -graphs to $Im T_{2 \rightarrow 2}$ appears to be controlled by two distributions: the distribution of complexities and a characteristic probability density \tilde{p} .

D Factoring K -Graphs From Chains

Here we demonstrate the steps leading to the factorization theorem illustrated in Fig. 9. For the purpose of this appendix let us assume that the diagram of Fig. 9a gives an N^{th} order contribution to $Im T_{2 \rightarrow 2}$ which we denote by

$$\begin{aligned} (Im T_{2 \rightarrow 2})_{\text{Fig. 9a}} &= \frac{g^2}{16\pi} \left(\frac{g}{16\pi^2} \right)^{N-2} \frac{1}{S} \int_0^1 \frac{dx_1 dx_2 \prod dy_i \prod dz_i}{U^2} \\ &\times \delta \left(1 - x_1 - x_2 - \sum y_i - \sum z_i \right) \left[\Theta \left(\frac{\phi}{U} - m^2 \right) + \Theta \left(-\frac{\phi}{U} - m^2 \right) \right]. \end{aligned} \quad (78)$$

We let y_i label the internal lines of the K -graph, x_1 and x_2 label the vertical lines connecting the K -graph to the rest of the graph, and the z_i label the internal lines of the circular blob. The second Θ -function in Eq. 78 assumes that Fig. 9a includes the appropriate u -channel exchange graph.

Let U' and ϕ' denote the functions of z_i which characterize the circular blob in Fig. 9a and let U_K and ϕ_K be the corresponding functions of y_i for the K -graph. If U and ϕ describe the whole graph, one can show that

$$\phi = s \frac{\phi_K}{s} \frac{\phi'}{s}, \quad (79)$$

and

$$U = U_K (x_1 + x_2) U' + R . \quad (80)$$

The remainder $R \geq 0$ is a polynomial with the property that if one introduces scaling variables for all the loops in the original graph then R is of higher order in the scaling variables (see Eqs. 13,14). Our strategy is to use Eqs. 79-80 to decompose U , the Θ -function and the δ -function in Eq. 78 in order to demonstrate factorization.

Since the dominant contributions to $Im T_{2 \rightarrow 2}$ come from the region where U vanishes, it is a good first approximation to drop R in Eq. 80 and use $U = U_K (x_1 + x_2) U'$ in the $1/U^2$ factor of Eq. 78. The sum of the Θ -functions may be rewritten as

$$\begin{aligned} \Theta\left(\frac{\phi}{U} - m^2\right) + \Theta\left(-\frac{\phi}{U} - m^2\right) &= \Theta\left(\frac{\phi'/s}{(x_1 + x_2)U'} - \frac{m^2}{s} \left| \frac{s}{\phi_K} \right| \left(U_K + \frac{R}{(x_1 + x_2)U'} \right) \right) \\ &+ (\phi' \rightarrow -\phi') . \end{aligned} \quad (81)$$

In the leading-log approximation the factor multiplying m^2/s in Eq. 81, namely,

$$\left| \frac{s}{\phi_K} \right| \left(U_K + \frac{R}{(x_1 + x_2)U'} \right) \quad (82)$$

may be absorbed into the definition of m^2 since any finite positive multiple of m^2 is equivalent to m^2 for the purpose of regulating potential logarithmic divergences of the circular blob. To see that the inherent properties of K -graphs ensure that the factor in Eq. 82 is well-behaved, imagine rescaling the Feynman parameters of an l -line loop of the K -graph by introducing into Eq. 78 the identity $1 = \int_0^1 d\lambda \delta(\sum_{i=1}^l y_i)$ and letting $y_i = \lambda \tilde{y}_i$. At worst, the factor of Eq. 82 scales as $\sim 1/\lambda$ for small λ , but this region is not weighted heavily since the overall λ -integral varies as $\int_0^1 \lambda^{l-3} d\lambda$ since K -graphs have no two-line loops. Consequently, absorbing the K -graph factor of Eq. 82 into the definition of m^2 amounts to writing

$$\begin{aligned} \Theta\left(\frac{\phi}{U} - m^2\right) + \Theta\left(-\frac{\phi}{U} - m^2\right) &\simeq \left[\Theta\left(\frac{\phi'/s}{(x_1 + x_2)U'} - \frac{m^2}{s}\right) + \Theta\left(-\frac{\phi'/s}{(x_1 + x_2)U'} - \frac{m^2}{s}\right) \right] \\ &\times \left[\Theta\left(\frac{\phi_K}{U_K}\right) + \Theta\left(-\frac{\phi_K}{U_K}\right) \right] \end{aligned} \quad (83)$$

where, for future reference, we suggestively include the second factor in square brackets which trivially sums to unity.

Turning finally to the δ -function of Eq. 78 we invoke the decomposition

$$\delta\left(1 - x_1 - x_2 - \sum y_i - \sum z_i\right) = \int_0^1 d\lambda \delta\left(\lambda - \sum y_i\right) \delta\left(1 - x_1 - x_2 - \lambda - \sum z_i\right) . \quad (84)$$

Substituting Eqs. 79–84 into Eq. 78 and changing variables to $y_i = \lambda \tilde{y}_i$ (i.e., simultaneously scaling all Feynman parameters of the K -graph) gives

$$\begin{aligned}
(Im\ T_{2 \rightarrow 2})_{\text{Fig. 9a}} &= \frac{g^2}{16\pi} \left(\frac{g}{16\pi^2} \right)^{N-2} \frac{1}{S} \int_0^1 \frac{\prod d\tilde{y}_i \delta(1 - \sum \tilde{y}_i)}{U_K^2(\tilde{y})} \\
&\times \int_0^1 \frac{d\lambda dx_1 dx_2 \prod dz_i \delta(1 - x_1 - x_2 - \lambda - \sum z_i)}{\lambda ((x_1 + x_2)U')^2} \\
&\times \left[\Theta \left(\frac{\phi'/s}{(x_1 + x_2)U'} - \frac{m^2}{s} \right) + \phi' \rightarrow -\phi' \right]
\end{aligned} \tag{85}$$

where the integral over \tilde{y}_i defines an overall multiplicative factor because

$$\frac{\prod dy_i}{U_K^2(y_i)} = \frac{\prod d\tilde{y}_i}{U_K^2(\tilde{y}_i)}, \tag{86}$$

is independent of λ . The integrals over λ, x_1, x_2 and z_i in Eq. 85 may be put in a familiar form by transforming from λ to the variables w_1 and w_2 through

$$\int_0^1 \frac{d\lambda}{\lambda} \delta(1 - x_1 - x_2 - \lambda - \sum z_i) = \int_0^1 \frac{dw_1 dw_2}{(w_1 + w_2)^2} \delta(1 - x_1 - x_2 - w_1 - w_2 - \sum z_i). \tag{87}$$

This transformation is most easily verified by inserting $1 = \int_0^1 d\lambda \delta(\lambda - w_1 - w_2)$ on the right-hand side and then performing a change of variables by defining $w_i = \lambda \tilde{w}_i$.

Before putting together all the above expressions, consider the graph of Fig. 9b (disregarding the factor \hat{K} which we will discuss below) obtained by replacing the K -graph of Fig. 9a with a two-line loop labelled by the Feynman parameters w_1 and w_2 . If we let ϕ'' and U'' denote the functions characterizing Fig. 9b then

$$\phi'' = w_1 w_2 \frac{\phi'}{s}, \quad U'' = (w_1 + w_2)(x_1 + x_2)U' + R'', \tag{88}$$

where the remainder R'' is analogous to that in Eq. 80. To leading-log accuracy the Θ -functions in Eq. 85 can be re-expressed in terms of ϕ'' and U'' because

$$\Theta \left(\frac{\phi'/s}{(x_1 + x_2)U'} - \frac{m^2}{s} \right) \simeq \Theta \left(\frac{\phi'/s}{(x_1 + x_2)U'} - \frac{m^2 (w_1 + w_2)}{s w_1 w_2} \right) = \Theta \left(\frac{\phi''}{U''} - m^2 \right) \tag{89}$$

Substituting Eqs. 87-89 into Eq. 85 we arrive at the final result

$$(Im\ T_{2 \rightarrow 2})_{\text{Fig. 9a}} = \hat{K} \times (Im\ T_{2 \rightarrow 2})_{\text{Fig. 9b}} \tag{90}$$

where for a N_K^{th} order K -graph,

$$\hat{K} \equiv \frac{(Im\ T_{2 \rightarrow 2})_K}{(Im\ T_{2 \rightarrow 2})_{N=2}} = \frac{\frac{g^2}{16\pi} \left(\frac{g}{16\pi^2}\right)^{N_K-2} \int_0^1 \frac{[d\tilde{y}]}{U_K^2}}{\frac{g^2}{16\pi} \frac{1}{2}} = 2 \left(\frac{g}{16\pi^2}\right)^{N_K-2} \int_0^1 \frac{[d\tilde{y}]}{U_K^2}. \quad (91)$$

The denominator $(Im\ T_{2 \rightarrow 2})_{N=2}$ in the definition of \hat{K} is simply the imaginary part of a single two-line loop.

The contribution of the graph of Fig. 9b is

$$\begin{aligned} (Im\ T_{2 \rightarrow 2})_{\text{Fig. 9b}} &= \frac{g^2}{16\pi} \left(\frac{g}{16\pi^2}\right)^{N-N_K-2} \frac{1}{2S} \int_0^1 \frac{dw_1 dw_2 dx_1 dx_2 \prod dz_i}{U'^2} \\ &\times \delta\left(1 - x_1 - x_2 - w_1 - w_2 - \sum z_i\right) \left[\Theta\left(\frac{\phi''}{U''} - m^2\right) + (\phi'' \rightarrow -\phi'') \right], \end{aligned} \quad (92)$$

where the factor of 2 accompanying the symmetry factor S (which describes Fig. 9a) accounts for extra two-line loop. To keep the discussion simple, we have implicitly assumed throughout the discussion that the isolated K -graph has a symmetry factor of unity.

One might wonder how general the analysis of Fig. 9 can be. It turns out that imaginary part of every graph we consider can be written, even with two legs off-shell, as a linear superposition of the the imaginary parts of one-loop graphs. Consider the graph of Fig. 13, where it is understood that the internal lines have mass M (not to be confused with any physical mass m). Note particularly that the momentum p' has been replaced by $\beta p'$, where β , it turns out, runs from -1 to 1 . Actually, only $\beta > 0$ contributes to the imaginary part, as we will see. The graph of Fig. 13 has the value (aside from an additive cut-off dependent contribution to its real part)

$$\int_0^1 dx \ln \left[M^2 - x(1-x)(-k + \beta p')^2 \right]. \quad (93)$$

Multiply this by a function $F(M^2, \beta)$, whose significance we reveal below, take the imaginary part, and integrate over $M^2 > 0$, $|\beta| \leq 1$; the result is

$$2\pi \int_0^\infty dM^2 \int_{-1}^1 d\beta F(M^2, \beta) \int_0^{1/2} dx \Theta \left[(-k + \beta p')^2 - \frac{M^2}{x(1-x)} \right] \quad (94)$$

In writing eq. 94 we have made use of the symmetry in x and $1-x$. Now change variables to

$$\rho^2 = \frac{M^2}{x(1-x)}, \quad dx = \frac{M^2}{\rho^4} d\rho^2 (\rho^2 - 4m^2)^{-1/2} \quad (95)$$

Then Eq. 94 becomes

$$\int_0^\infty d\rho^2 \int_{-1}^1 d\beta h(\rho^2, \beta) \Theta \left[(-k + \beta p')^2 - \rho^2 \right] \quad (96)$$

with

$$h(\rho^2, \beta) = \frac{2\pi}{\rho^4} \int_0^{\rho^2/4} dM^2 M^2 F(M^2, \eta) \left(\rho^2 - 4M^2 \right)^{-1/2}. \quad (97)$$

This relation between h and F is Abel's integral equation which can be explicitly solved.

The significance of Eq. 96 is that it is a general representation[28, 29] of the imaginary part of the Feynman graphs we consider; we call it (following ancient usage[30]) the DGS representation. It is a form of the Jost-Lehmann-Dyson representation which can be derived either by appealing to causality and spectrum conditions[28], or by direct investigation of Feynman-parameter representations of graphs[29]. The DGS representation reduces the analysis of general graphs to a linear superposition of Fig. 13 (with $p' \rightarrow \beta p'$). We note that the physical region of $\text{Im } T(-k, \beta p')$ is restricted by the requirement $-k_0 + \beta p'_0 \geq 0$, which turns out to mean $\beta \geq 0$. This is just telling us that $\text{Im } T$ receives contributions from parts involving $\ln(-s/m^2)$, not $\ln(-u/m^2)$.

E Bounds From Beyond K -graphs

Our estimates of the contributions of pure K -graphs (and their exchange graphs) to $\text{Im } T_{2 \rightarrow 2}$ involved the complexity density function multiplied by the total number of K -graphs. In this section we extend our estimates by considering an even larger class of graphs without logarithms which encompasses both K -graphs, their exchange graphs, and s -channel graphs.

Of use to us is a combinatorial result of Bender and Canfield[18] who obtained an expression for the asymptotic number of labelled graphs with a specified number of lines attached to each vertex. In particular we are interested in the number of N^{th} order ϕ^4 graphs with 4 external legs such that the graphs have neither tadpoles nor multiple lines between vertices — these criteria ensure the absence of logarithms in the corresponding contributions to $\text{Im } T_{2 \rightarrow 2}$. The number of labelled graphs with the desired properties is asymptotically equal to

$$\frac{(4N+4)!}{(2N+2)!} \frac{1}{2^{2N+2}} \frac{1}{(4!)^N} \exp \left[-\frac{3N}{2(N+1)} - \left(\frac{3N}{2(N+1)} \right)^2 \right] \doteq \left(\frac{2}{3} \right)^N (N!)^2. \quad (98)$$

Converting from the language of labelled graphs to the the usual implementation of the Feynman rules which employs unlabeled graphs amount to dividing the Eq. 98 by $N!$ so

that the effective number of diagrams without logarithms is $\doteq (2/3)^N N!$. For example, the corresponding bound on $Im\ T_{2\rightarrow 2}$ analogous to Eq. 70 is obtained simply by replacing $N!/2^N$ (the number of K -graphs) with $(2/3)^N N!$ to obtain $a \geq 2/3$ in

$$Im\ T_{2\rightarrow 2} \doteq N! \left(\frac{ag}{16\pi^2} \right)^N. \quad (99)$$

If, as in Appendix B, we speculate about further improving the bounds on a by a factor of $(C_S/\langle C_i \rangle)^2 \simeq (32/27)^2$ (assuming that the average complexity of K -graphs is the same as the average complexity of all simple graphs) we obtain $a \simeq 2048/2187 \simeq 0.94$.

Figure Captions

1. A multiperipheral or straight-ladder graph for $2 \rightarrow 2$ scattering in $g\phi^4$ theory. In this and all other figures of this paper $g\phi^4$ vertices are indicated by dots.
2. Free ends of opposing multiperipheral tree graphs may be joined in all possible ways to generate generalized $2 \rightarrow 2$ amplitudes.
3. a) An eighth-order graph with no two-line loops. b) The u -channel exchange graph corresponding to a). c) Redrawn version of b) indicates that the u -channel exchange graph is not of the form of an eighth-order K -graph.
4. a) A fourth-order crossed-ladder graph b) The u -channel exchange graph corresponding to a).
5. a) The simplest example of a K -graph. b) Sixth-order graph containing a two-line loop and a K -graph. c) Eighth-order graph containing a K -graph crossed by two-line loops.
6. Two decay-like Cayley trees emerge from the point where p and p' meet. Summing over all such amplitudes and squaring contributes to the two-particle total cross section and $Im\ T_{2\rightarrow 2}$.
7. A $2 \rightarrow 2$ chain graph formed by linking together arbitrary combinations of K -graphs and two-line loops.
8. Graphical representation of the Bethe-Salpeter equation which sums all of amplitudes of the form shown in Fig. 7. The circular blobs include the corresponding u -channel exchange graphs.

9. Illustration of the factorization theorem which permits replacement of a K -graph in a chain graph with a two-line loop and a numerical factor \hat{K} given by Eq. 33. The circular blob is assumed to include contributions from u -channel exchange graphs.
10. Distribution of the complexity for all 43,200 K -graphs for $N = 14$.
11. Comparison of the asymptotic form of Eq. 51 with numerical integration of $\int_0^1 [dx]/U_S^2$.
12. Histograms show the probability density of $U/\langle U \rangle_i$ for all 72 eighth-order K -graphs. The vertical dark bands are a consequence of the similarity between the distributions in addition to fluctuations in the Monte-Carlo calculation of each histogram. Solid curve shows the corresponding distribution for the completely symmetric function U_S .
13. The off-shell two-line loop whose weighted sum appears in the DGS representation.

References

- [1] A. Ringwald, Nucl. Phys. **B330**, 1 (1990).
- [2] O. Espinosa, Nucl. Phys. **B343**, 310 (1990).
- [3] N. Manton, Phys. Rev. **D28**, 2019 (1983); F Klinkhamer and N. Manton, Phys. Rev. **D30**, 2212 (1989).
- [4] J.M. Cornwall, Phys. Lett., **B243**, 271 (1990).
- [5] L.N. Lipatov, Pis'ma Zh. Eksp. Teor. Fiz., **24**, 179 (1976) [JETP Lett., **24**, 157 (1976)].
- [6] E. Brézin, J.C. le Guillou and J. Zinn-Justin, Phys. Rev. **D15**, 1544 (1977); **15**, 1558 (1977). For other references, see J.C. le Guillou and J. Zinn-Justin, eds., *Large-Order Behavior of Perturbation Theory*, Current Physics Sources and Comments, Vol. 7, (North-Holland, Amsterdam, 1990).
- [7] H. Goldberg, Phys. Lett., **B246**, 445 (1990); Phys. Rev. **D45**, 2945 (1992); M. Voloshin, Phys. Rev. **D43**, 1726 (1991).
- [8] V.I. Zakharov, Nucl. Phys. **B377**, 501 (1992).

- [9] The literature on multiperipheralism is vast. Some of the original works and works useful to use are: D. Amati, A. Stanghellini and S. Fubini, *Nuovo Cim.* **26**, 896 (1962); M. Baker and I Muzinich, *Phys. Rev.* **132**, 2291 (1963); S. Nussinov and J. Rosner, *J. Math. Phys.*, **7**, 1670 (1966).
- [10] R.F. Sawyer, *Phys. Rev.* **131**, 1384 (1963); I.F. Ginzburg and V.V. Serebryakov, *Yad. Fiz.* **3**, 164 (1966) [*Sov. J. Nucl. Phys.* **3**, 115 (1966)].
- [11] B.A. Arbuzov and V.E. Rochev, *Yad. Fiz.* **23**, 904 (1976) [*Sov. J. Nucl. Phys.* **23**, 475 (1976)].
- [12] J.M. Cornwall and G. Tiktopoulos, *Phys. Rev.* **D45**, 2105 (1992).
- [13] M. Mattis, *Phys. Rep.* **214**, 159 (1992).
- [14] see e.g., H. Cheng and T.T. Wu, *Expanding Protons: Scattering at High Energies*, (MIT Press, Cambridge, MA, 1987).
- [15] H. Verlinde and E. Verlinde, *Nucl. Phys.* **B371**, 446 (1992); Princeton preprint PUPT-1319, hep-ph 9302104, Sept. 1993 (unpublished).
- [16] C.M. Bender and T.T. Wu, *Phys. Rev. Lett.* **37**, 58 (1976).
- [17] G. Parisi, *Phys. Lett.* **68B**, 117, (1977).
- [18] E.A. Bender and E.R. Canfield, *J. of Comb. Th.*, **A24**, 296 (1978).
- [19] Y. Shimamoto, *Nuovo Cim.* **25**, 1292 (1962); G. Tiktopoulos, *Phys. Rev.* **131**, 450 (1963); P. Federbush and M. Grisaru, *Ann. Phys. (NY)* **22**, 263 (1963); J. Polkinghorne, *J. Math. Phys.* **4**, 503 (1963); I.G. Halliday, *Nuovo Cim.* **30**, 177 (1963); N. Nakanishi, *Graph Theory and Feynman Integrals*, (Gordon and Breach, New York, 1971).
- [20] B. Bollobás, *J. London Math. Soc. (2)* **26**, 201 (1982).
- [21] see e.g., G.H. Hardy, J.E. Littlewood and G. Pólya, *Inequalities*, (Cambridge University Press, London, 1952).
- [22] N. Biggs, *Algebraic Graph Theory* (Cambridge University Press, Cambridge, 1974).

- [23] Cheng and Wu, Ref. 11 and references therein; also, J.M. Cornwall and G. Tiktopolous, in *New Pathways in High-Energy Physics II*, ed. A. Perlmutter (Plenum, New York, 1976) p. 213; F. Zachariasen and P. Carruthers, *ibid.* p. 265.
- [24] A fictitious mass is inserted by hand to regulate IR divergences. In fact, the QCD gluon has a non-perturbative constituent mass, just as quarks do (J.M. Cornwall, Phys. Rev. **D26**, 1453 (1982).) To what extent it is accurate just to put a constituent mass into perturbative diagrams is not known.
- [25] A. De Rújula, Phys. Rev. Lett. **32**, 1143 (1974); D. Gross and S.B. Treiman, Phys. Rev. Lett. **32**, 1145 (1974); J.M. Cornwall and G. Tiktopolous, Phys. Rev. Lett. **35**, 338 (1975).
- [26] J.M. Cornwall and G. Tiktopolous, Ann. Phys. (NY) **228**, 365 (1993); N. Hatzigeorgiu and J.M. Cornwall, Phys. Lett. **B327** 313 (1994).
- [27] H.N.V. Temperley, Proc. Phys. Soc. **83** 3 (1964).
- [28] S. Deser, W. Gilbert, and E.C.G. Sudarshan, Phys. Rev. **115**, 731 (1959).
- [29] N. Nakanishi, Prog. Theo. Phys. (Kyoto) **23**, 1151 (1960).
- [30] J.M. Cornwall and R.E. Norton, Phys. Rev. **173**, 1637 (1968).

Table 1 Average complexity of N^{th} order K -graphs. Up to $N = 12$ C is calculated for all $(N/2)!(N/2 - 1)!/2$ graphs but for larger N , due to practical limitations of computer time, only a reasonable number of randomly generated graphs are averaged over.

N	$\langle C \rangle$	$\sqrt{\langle C^2 \rangle - \langle C \rangle^2}$	# graphs
4	16	0	1
6	1.29×10^2	1	6
8	1.13×10^3	6.78×10^1	72
10	1.04×10^4	8.89×10^2	1440
12	9.96×10^4	1.01×10^4	43200
20	1.02×10^9	1.34×10^8	10000
30	1.32×10^{14}	1.91×10^{13}	10000
40	1.90×10^{19}	2.90×10^{18}	10000
50	2.92×10^{24}	4.67×10^{23}	10000
60	4.67×10^{29}	7.53×10^{28}	10000
70	7.66×10^{34}	1.25×10^{34}	10000
100	3.80×10^{50}	6.43×10^{49}	5000
200	1.28×10^{103}	2.20×10^{102}	500
300	5.67×10^{155}	9.66×10^{155}	500
400	2.96×10^{208}	5.15×10^{207}	500

This figure "fig1-1.png" is available in "png" format from:

<http://arxiv.org/ps/hep-ph/9408274v1>

This figure "fig1-2.png" is available in "png" format from:

<http://arxiv.org/ps/hep-ph/9408274v1>

This figure "fig1-3.png" is available in "png" format from:

<http://arxiv.org/ps/hep-ph/9408274v1>

This figure "fig1-4.png" is available in "png" format from:

<http://arxiv.org/ps/hep-ph/9408274v1>

This figure "fig1-5.png" is available in "png" format from:

<http://arxiv.org/ps/hep-ph/9408274v1>

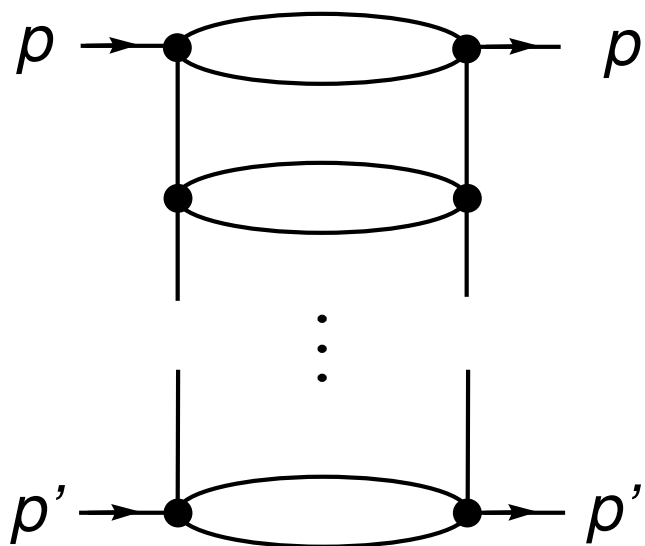


Fig. 1

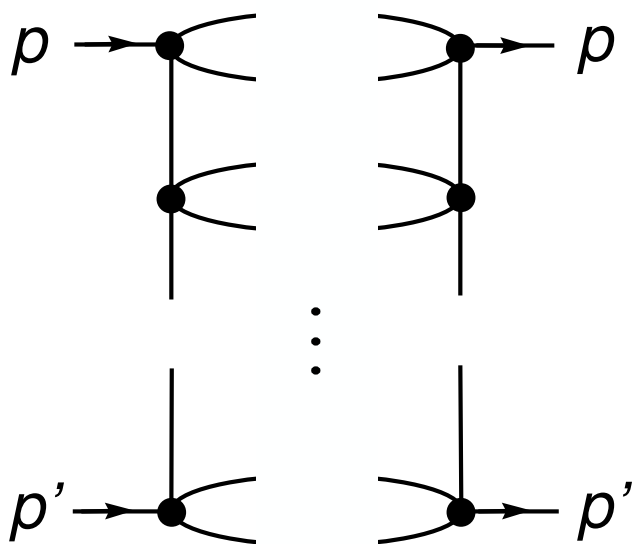
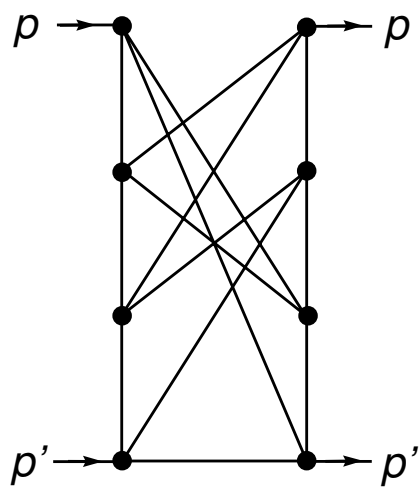
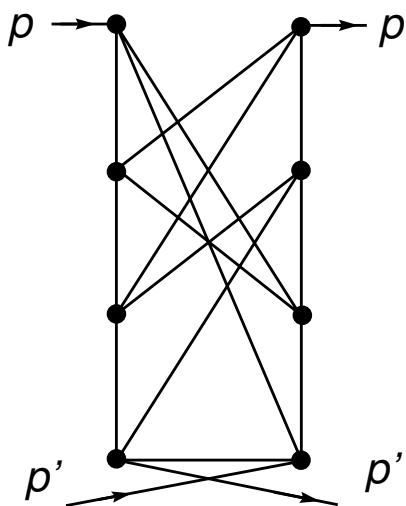


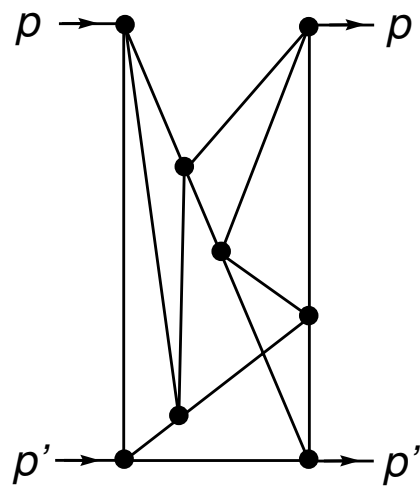
Fig. 2



(a)

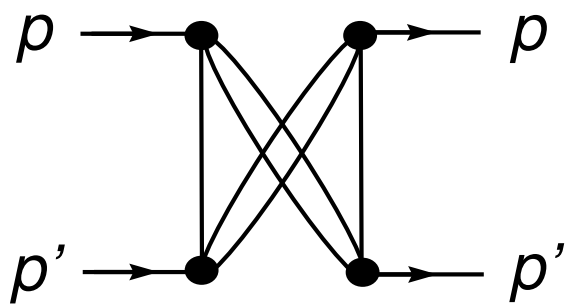


(b)

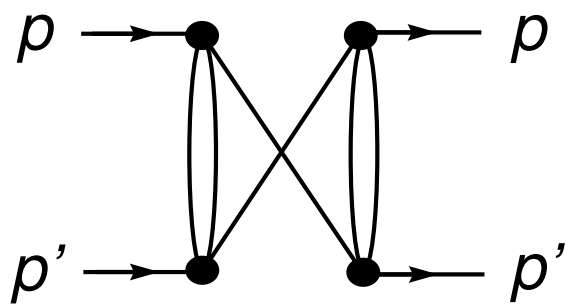


(c)

Fig. 3

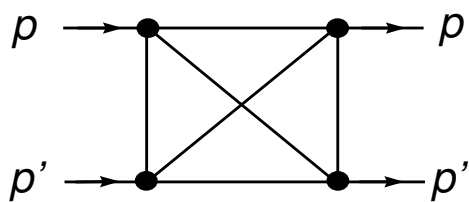


(a)

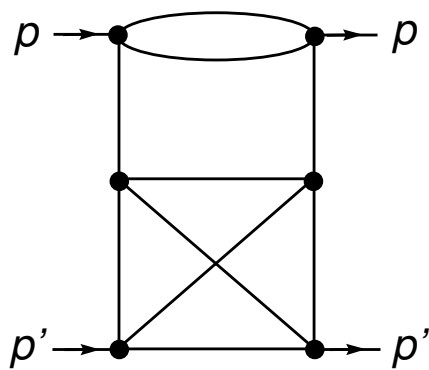


(b)

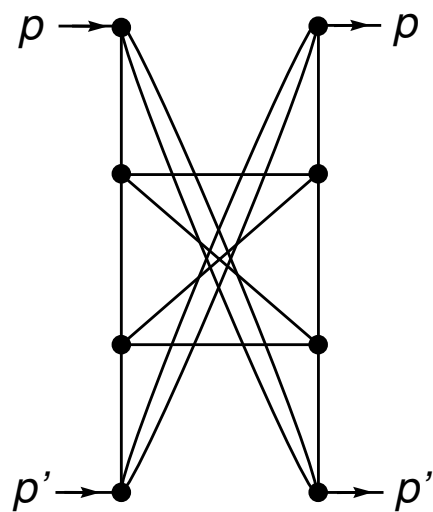
Fig. 4



(a)



(b)



(c)

Fig. 5

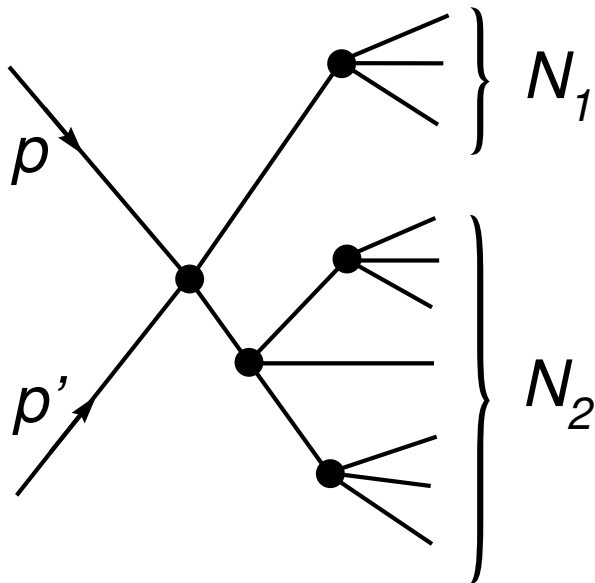


Fig. 6

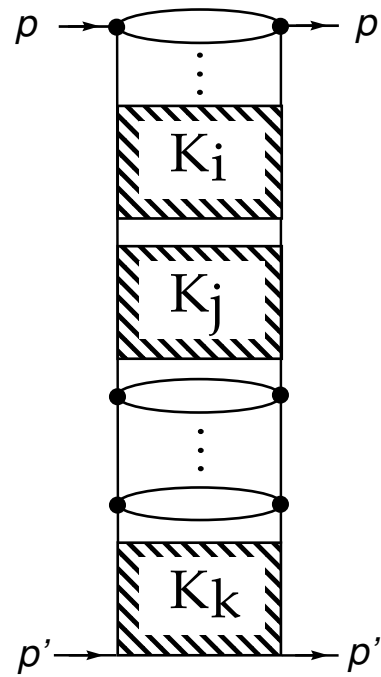


Fig. 7

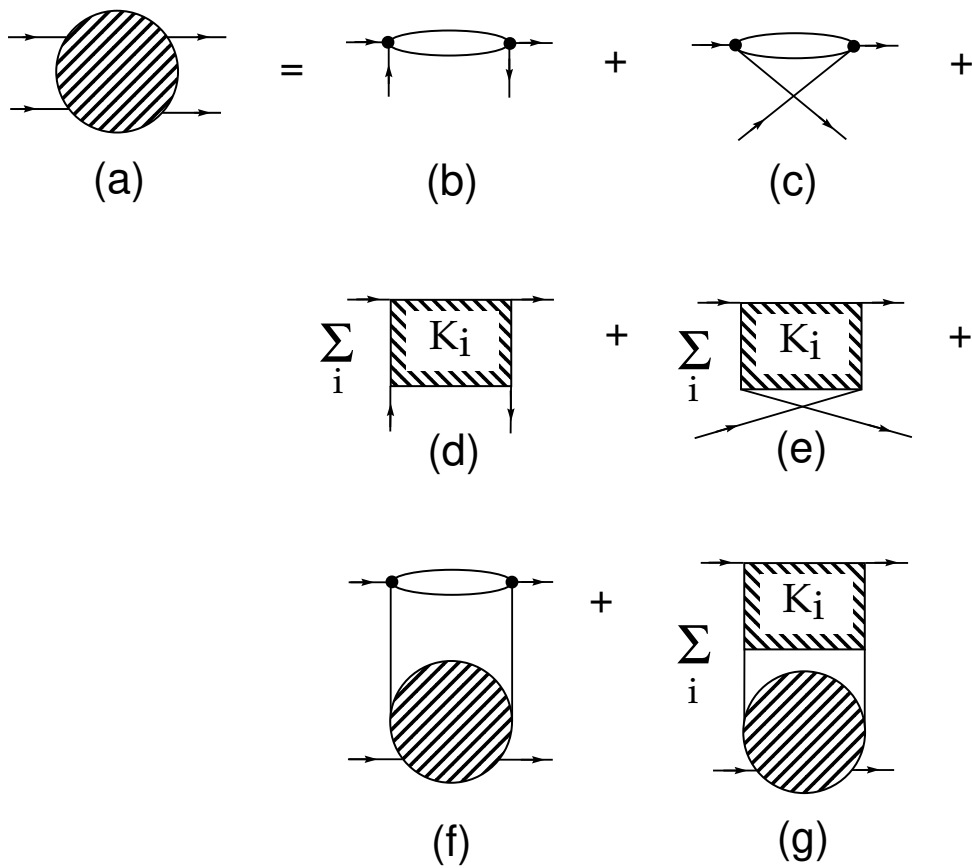


Fig. 8

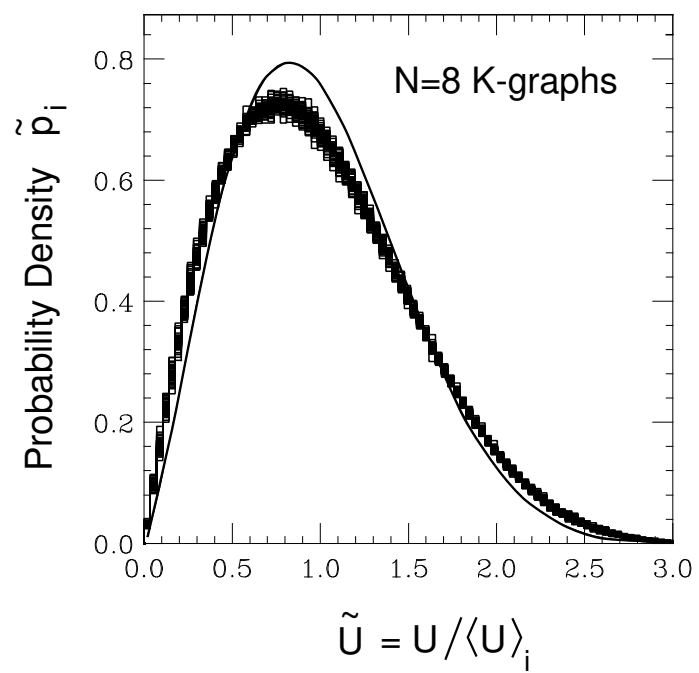


Fig. 12

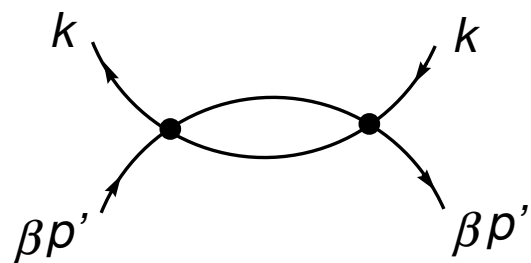


Fig. 13

